NURETH14-132

Subchannel and rod bundle PSBT simulations with Cathare 3

M. Valette

Commissariat à l'Énergie Atomique et aux Énergies Alternatives, DEN, DER/SSTH, F-38054 Grenoble, France

Abstract

This paper presents the assessment of CATHARE3 against PWR subchannel and rod bundle tests of the PSBT benchmark. Noticeable measurements were the following: void fraction in single subchannel and rod bundle, multiple liquid temperature at subchannel exit in rod bundle, DNB power and location in rod bundle. All these results were obtained both in steady and transient conditions.

Void fraction values are satisfactory predicted by CATHARE3 in single subchannels with the pipe module. More dispersed predictions are obtained in rod bundles with the 3D module at subchannel scale. Single phase liquid mixing tests and DNB tests in rod bundle are also analyzed.

Introduction

CATHARE 3 is a new two phase thermalhydraulics system code developed at CEA Grenoble (ref. [1]). It is designed to expand the capabilities of CATHARE 2 and to improve the simulation accuracy of light water reactor accidents. New features include additional fields, like a droplet field or a bubble field, and coupled equations of turbulence transport for a continuous field or interfacial area transport for a dispersed field. Beside the unchanged choices for numerical schemes for time and space discretization, a numerical solver gathering the different modules of a circuit has been rewritten and improved compared to CATHARE 2 in order to allow new capabilities of coupling with external codes, for example for neutronics, or detailed CFD. The preliminary version V1 needs a wide validation program. This paper deals with the 1D and 3D module validation of the code against various experiments at subchannel scale.

Following the BWR Full-size Fine-Mesh Bundle tests (BFBT) benchmark, the PWR subchannel and bundle tests (PSBT) benchmark (ref. [2]) is proposed by OECD/NRC. Both are based upon a NUPEC data base obtained in full scale subchannels and rod bundles and include detailed measurements of fluid temperature, void fraction and critical power or DNB power in steady and transient conditions. These experiments are useful to check and validate the code closure laws in rod bundles, especially the turbulence dispersion coefficients for heat in single phase flow and void in two phase flow, the wall and interfacial friction coefficients and the wall-to-fluid heat transfer models. The PSBT phase I exercises are devoted to the void fraction measurements, performed in single subchannels and in 5x5 rod bundles in steady and transient conditions. In the first exercise, phase II features liquid temperature measurements in all subchannels of a heterogeneously heated rod bundle in steady conditions, and, in the following exercises, DNB measurements taken in various rod bundles in steady and transient conditions, i.e. power value and location of first detected DNB.

Single subchannel experiments are simulated by the CATHARE 3 pipe 1D module while rod bundle cases are simulated with the CATHARE 3 3D module meshed at a subchannel scale, i.e. one cell per subchannel in a horizontal cross cut.

Useful balance equations and closure laws are briefly presented in the following section 1. Then, results of comparisons between simulations and measurements of void fraction for Phase I exercises are presented in section 2. The results of temperature and DNB simulations of Phase II exercises are presented in section 3.

1. CATHARE 3 balance equations and closure laws

Contrary to the preceding BFBT simulations (ref. [3]), featuring high void two phase flow, most of the PSBT benchmark data base remain in the low void range and hence, simulations do not need an additional droplet field beside the standard 6-equation model.

For a given generation of steam along a single heated channel, the local void fraction is governed by wall and interfacial friction. In a 3D flow inside a rod bundle, cross-flows between adjacent subchannels lead to void dispersion. Also turbulent dispersion or diffusion may affect the temperature map in the single phase region. The void dispersion phenomena can be modelled by a mixing term in the momentum balance equations. The temperature dispersion (caused by non random flow from one subchannel to a neighbour) and diffusion (caused by random fluctuations of flow between adjacent subchannels) are modelled by a single term in the liquid energy balance equation. The velocity diffusion is presently neglected in the momentum equation.

Momentum balance

$$\alpha_{k} \rho_{k} \left[\frac{\partial}{\partial t} V_{k} + V_{k} \cdot \nabla V_{k} \right] = -\alpha_{k} \nabla P + p_{i} \nabla \alpha_{k} + (-1)^{k} t_{i} + t_{pk} + \alpha_{k} \rho_{k} g$$

Wall frictions of both phases are calculated using the Blasius friction coefficient f_k multiplied by a phase-dependant multiplier c_k .

$$t_{pk} = \chi c_k f_k \rho_k \frac{|V_k| V_k}{2} \quad \text{with } c_g = \alpha^{1.25} \quad \text{and} \quad c_l = \frac{(l-\alpha)\rho_l}{(l-\alpha)\rho_l + \alpha \rho_g}$$

Interfacial friction in bubbly, slug and churn vertical flow is given by

$$t_{i} = \frac{K_{l} \rho_{l} + K_{g} \rho_{g}}{L} \alpha (1 - \alpha)^{3.6} [V_{g} - V_{l}]^{2}$$

L is the maximum bubble size, limited by the Laplace length $\ell = \sqrt{\frac{\sigma}{g(\rho_l - \rho_s)}}$ and the hydraulic

diameter

$$K_g = 29$$

$$K_{l} = (F_{\mu})^{0.25} f_{l}$$
 with $F_{\mu} = \frac{\mu_{l}}{\sqrt{\rho_{l} \sigma \ell}}$ and $f_{l} = 2.81 + 34(L/D_{h})^{5} (6 - 5L/D_{h})$

 $t_{i} \mbox{ and } t_{p} \mbox{ are unchanged compared to CATHARE 2 6 equation model.}$

The mixing term p_i is calculated from an assessment of the turbulent kinetic energy.

For a single phase flow in a tube or a subchannel (far from a spacer grid), the turbulent kinetic energy $k_{\rm l}$ can be assessed by:

$$k_1 = 0.0367 V_{,2} Re^{-1/6}$$
 (see ref. [4])

The associated turbulent viscosity can be assessed as:

$$v_{t} = 0.5D_{H}\sqrt{k_{t}}$$

and the dispersion term pi:

$$p_i = 0.4 \; \mu_t \; \frac{V_l}{D_H}$$

The coefficient 0.4 comes from an order of magnitude for the velocity gradients between subchannels; the velocity difference is evaluated at 40% of the axial velocity, which is close to the velocity module. At the end, it comes:

$$p_i = 0.038 \, \rho_i \, V_i^2 Re^{-1/12}$$

The coefficient 0.5 in the v_t formula has been adjusted so as to better match the void fraction measurements in the PSBT Phase I tests. This coefficient appears to be several orders of magnitude above the figure calculated using simple turbulence (ref. [4] and [5]); the void dispersion due to cross flows (and not only diffusion) seems to be the main driving phenomena (see ref. [6]).

Continuous liquid energy balance

It is written in internal energy for the 3D module as follows:

$$\frac{\partial}{\partial t} (\alpha_{l} \rho_{l} e_{l}) + \nabla \cdot (\alpha_{l} \rho_{l} e_{l} V_{l})$$

$$= q_{li} + \chi_{c} q_{pl} - \Gamma H_{lc} - P \left[\frac{\partial \alpha_{l}}{\partial t} + \nabla \cdot (\alpha_{l} V_{l}) \right] + \nabla \cdot \left[\alpha_{k} \left(\lambda_{l} T_{l} + \frac{\rho_{l} V_{ll}}{P r_{i}} \nabla e_{l} \right) \right]$$

The molecular diffusion is neglected compared to the turbulent diffusion term.

The departure from nucleate boiling appears on a hot wall when the heat flux towards the fluid exceeds the so called "critical heat flux", which is assessed in six equation model of CATHARE 2 and 3 using look up tables, given the local values of mass velocity, pressure and steam quality.

Nomenclature for equations

Roman letters

- c wall friction phase multiplier
- e internal energy
- f wall friction coefficient
- g gravity
- H enthalpy
- k turbulent kinetic energy
- K interfacial friction coefficient
- *l* Laplace length
- P pressure

- p_i void dispersion coefficient
- Pr Prandtl number
- q heat flux
- t time
- t_i interfacial stress
- t_p wall stress
- q heat flux
- T temperature
- V velocity

Greek letters

- α phase volume fraction
- Γ boiling/condensation rate
- χ friction area (or heated area) over control volume
- λ molecular heat conductivity
- μ dynamic viscosity
- ν kinematic viscosity
- ρ phase density
- σ surface tension

Indexes

- i interface
- k any phase
- liquid phase
- p wall
- t turbulent

2. Void fraction in PSBT Phase I exercises

2.1 Exercise I.1 Steady state in single subchannels

Four different geometries of single subchannels, for central, side and corner locations (side and corner are relative to a rod bundle in a square box) have been tested, resulting in void fraction measurements at 1400mm level inside a 1555mm long heated subchannel. They fit to standard PWR rod bundle subchannel geometry, with an additional test section corresponding to a central subchannel heated by 3 and not 4 contributing rods, one rod being replaced by a thimble. The CT scanner gives for every steady run a detailed void fraction array through the measuring section. Results can be compared with CFD simulations or averaged over the cross section for comparisons with 1D module simulation by system codes.

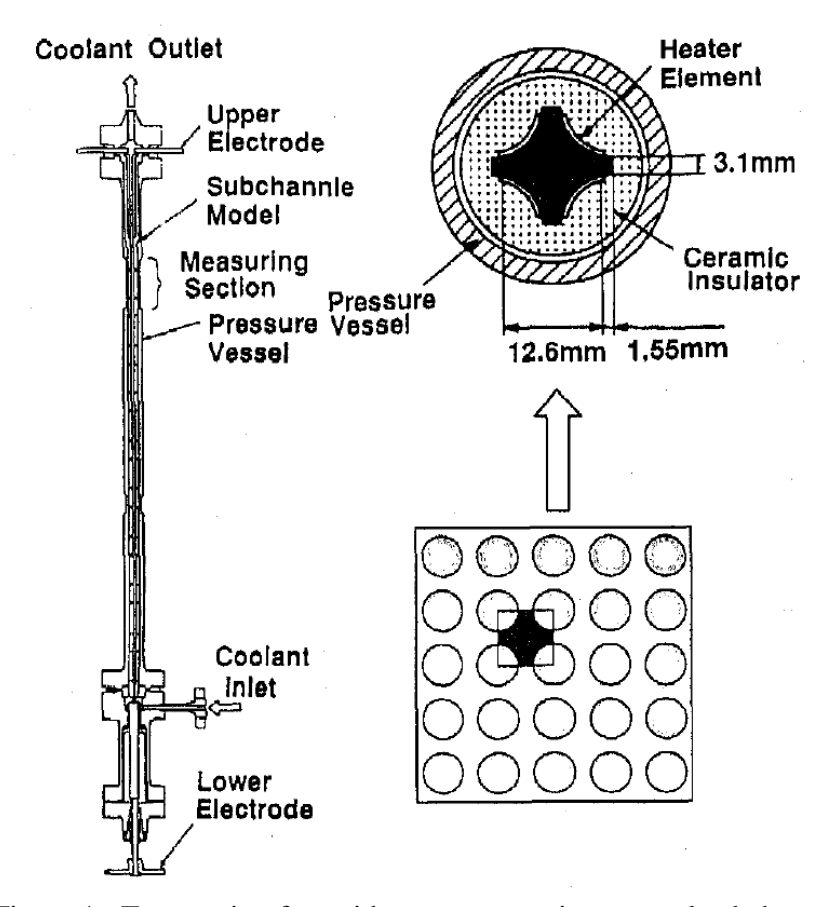


Figure 1: Test section for void measurement in a central subchannel

A set of 39 tests is proposed in the benchmark among a large data base of 126 tests. We calculated the whole data base and we compared the simulation results with the measurement data. Calculations were performed using a nearly uniform 31 cell meshing.

The results are gathered in the figure 2. One can see a good coherence, but yet a light bias, negative in any series, and a medium dispersion of the predicted values. The depicted experimental error bar is +/-4%. Some rare points are outside the range +/- 10%. The result statistics is presented in the table 1, given in % of void for the difference "predicted minus measured fraction".

	Nb tests	Average	Standard dev.
Series 1 : standard central subchannel	43	-2.3%	4.8%
Series 2 : central subchannel close to thimble	43	-1.8%	5.3%
Series 3 : lateral subchannel	20	-3.0%	6.0%
Series 4 : corner subchannel	20	-5.4%	3.2%
All series	126	-2.7%	5.0%

Table 1 : Distribution of deviations : « calculated minus measured void fraction» in the different series of single subchannel PSBT tests

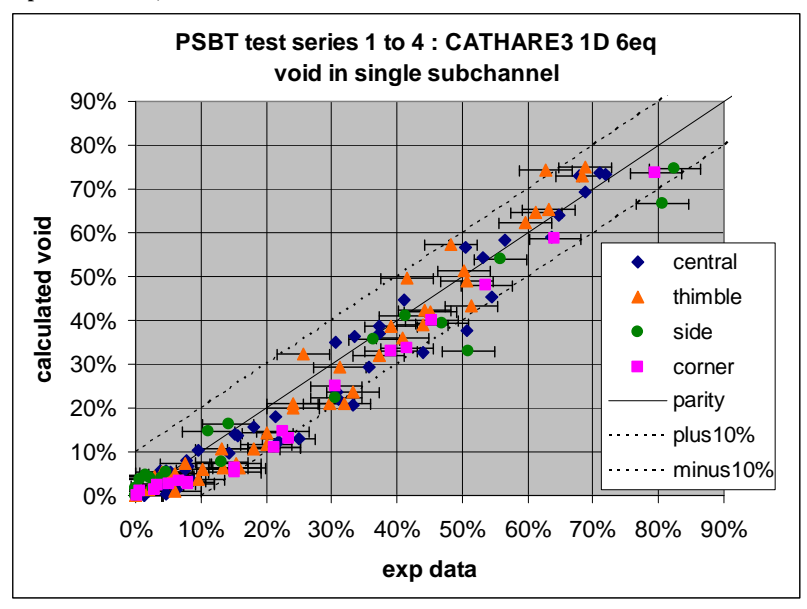


Figure 2 : PSBT single subchannel test comparison (thimble means a central subchannel close to an unheated thimble)

2.2 Exercise I.2 Steady state in rod bundles

Several types of rod bundles were tested, most of them including a 5x5 matrix of rods settled with 17 spacer grids of 3 different types, with uniform or cosine power profile and with or without a central thimble instead of a heated rod. The heated length was 3658mm, the rod diameter and pitch were 9.5 and 12.6mm.

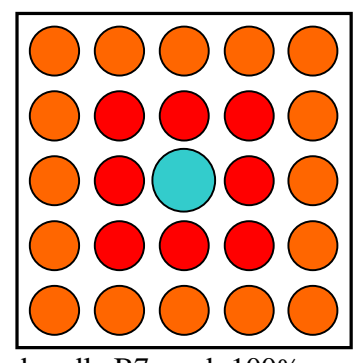


Figure 3: Power distribution in the bundle B7: red:100%, orange:85%, blue: unheated thimble

The heated part of the rod bundle was modelled by a 3D grid, with 6x6 cells in the x-y directions (one cell per subchannel). In the vertical direction, the height of each of the 17 spacer grids corresponded to a cell and the height between two following grids was divided into 3 cells, giving a total of 66 axial cells. The 3 different kinds of spacer grid were modelled by giving their porosity, hydraulic diameter and pressure loss coefficient due to the accurate restricted area in every subchannel.

An array of void fraction values in the different subchannels was measured at 3 different levels along the upper part of the heated length, reconstructed by 6 chordal averaged values in x and 6 in y directions. Only the averaged value of the 4 central subchannel void fractions was available in the

benchmark data base and this is the compared data versus the void calculated by CATHARE3 hereafter for all the tests of the benchmark.

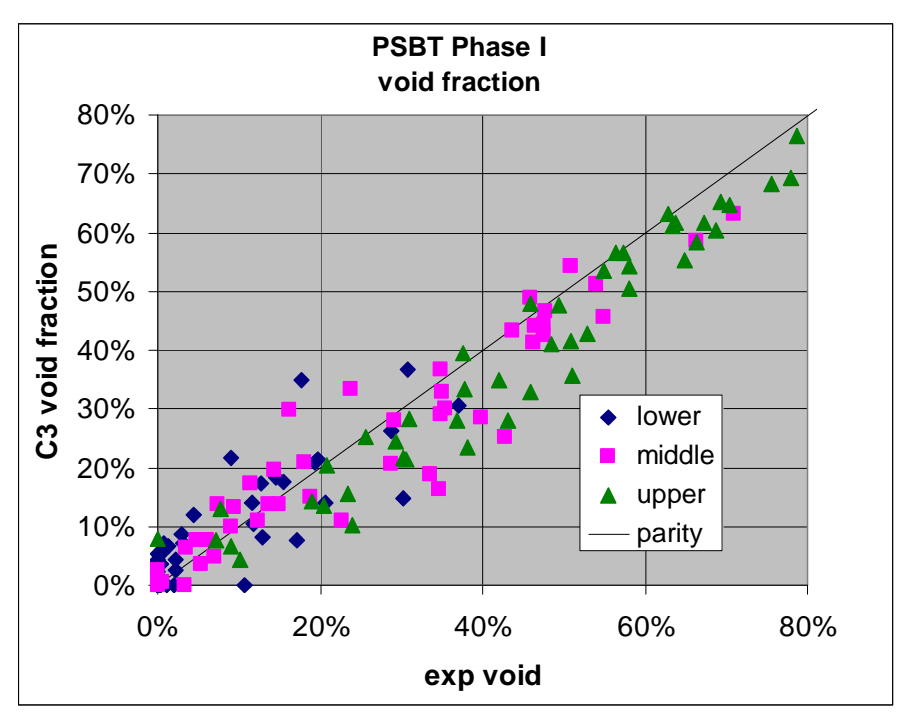


Figure 4 : PSBT rod bundle test comparison of predicted and measured void fraction at 3 different elevations along the heated length; lower : 2216mm; medium : 2669mm; upper : 3177mm

The points are more dispersed than for the single subchannel tests. The statistics of the results (difference: computed minus measured void fraction given in absolute %) is presented in the following table 2:

series	5	6	7	8	all mixed
Power profile	uniform	cosine	cosine	uniform	
Central thimble	no	no	yes	no	
Nb tests	11	11	12	11	45
average	-0.22%	-2.39%	1.13%	-6.65%	-1.96%
standard deviation	4.27%	5.43%	5.64%	6.73%	6.32%

Table 2 : PSBT rod bundle comparison statistics for void fraction tests

The series number correspond to 3 different bundles; the series 8 is tested with the same bundle as series 5 as repeated cases, which appear to be less satisfying.

2.3 Exercise I.3 Transient in rod bundles for void fraction prediction

A set of 12 transient tests is proposed in the benchmark, including power increase, flow reduction, temperature increase and depressurization in each of the 3 same tested bundles as in the steady tests of the exercise 2. The void fraction was also measured at the same 3 elevations during the transient. An example of comparison is given below for the test 7TPI, in the bundle B7 (with a central thimble and a

cosine power profile and given a linear increase of power, keeping constant the flow rate, pressure and inlet temperature. The void fraction is slightly underpredicted at the upper location but is satisfactory in front of the 2 lower void measurement elevations. The other tests show less satisfactory results, the upper and medium level void often remaining underpredicted.

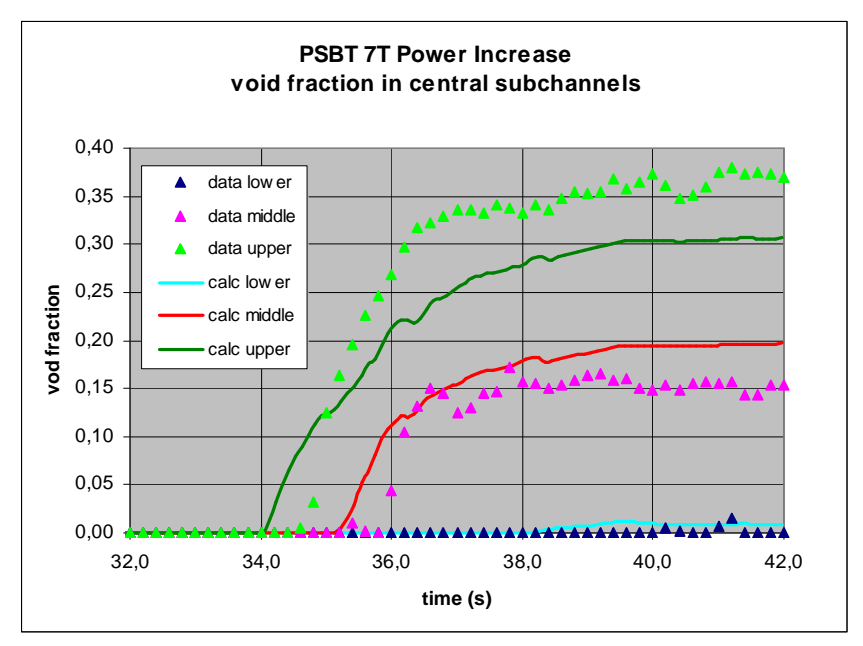


Figure 5 : Comparison of void fraction transient predicted by CATHARE 3 and measured in PSBT 7TPI test

3. Departure from Nucleate Boiling in PSBT Phase II exercises

3.1 Exercise II.1 Steady state fluid temperature in rod bundles

This exercise is particularly useful to assess the code capabilities for turbulent dispersion and diffusion in single phase flow.

In a 5x5 rod bundle featuring an heterogeneous power distribution (figure 4), a set of 36 thermocouples measure fluid temperature in every subchannel 50cm above the top of the heated length.

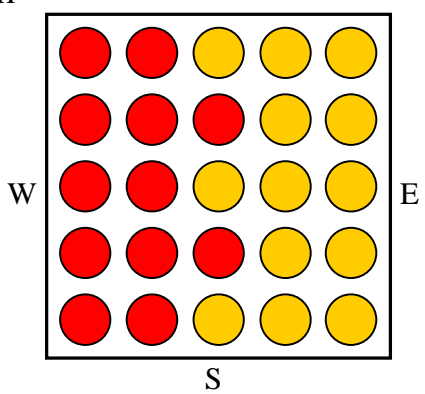
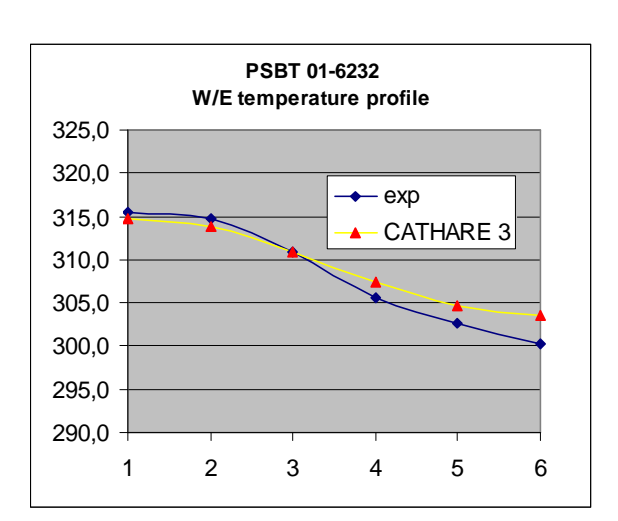


Figure 4 : Rod power distribution in fluid temperature measurement tests ; red rod power 100%, yellow 25%

Nine tests at high pressure (from 50 to 170 bars) are proposed for simulations in a wide range of mass fluxes (between 2. and 17.10⁶ kg/m²hr). The compared W/E profiles of temperatures, averaged in the N/S direction, are presented in the following figure 5. The x axis numbers correspond to the subchannel columns 1 to 6. The shown temperature gradient is due to the power distribution and is governed by the diffusion and dispersion across the subchannels.



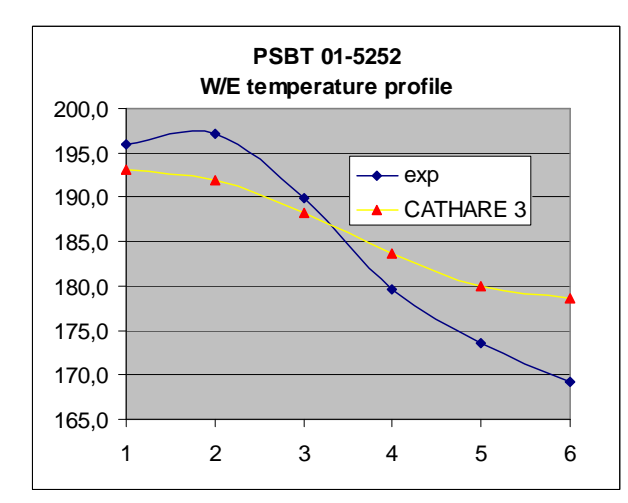


Figure 5: Temperature profiles in 2 fluid temperature measurement tests

Test number	Pressure	Mass flux	Inlet temperature	Power
	(kg/cm ² a)	$(10^6 \mathrm{kg/m^2 hr})$	(°C)	(MW)
01-6232	1691	2.10	251.5	0.42
01-5252	150.0	1.95	113.9	0.41

Table 2: Test parameters for temperature measurements

The profiles of half of the proposed tests are correctly predicted. The other tests show unbalanced measured temperatures at the outlet compared to inlet flow parameters and bundle power and hence, comparisons are not reasonable.

In the preceding table 2, the parameters of two correct tests are very close except the inlet temperature (which obviously may have a slight effect on the Reynolds number). However, the temperature profiles show unexplained different behaviours, which are not predicted by CATHARE 3.

3.2 Exercise II.2 Steady state DNB in rod bundles

As for the void fraction tests proposed in the phase I, different bundles were tested. The DNB is detected both in experiments and simulation by a significant rise of the wall temperature when the bundle power is slowly increased.

We calculated 3 test series in the bundles A2, A4 and A8, corresponding to a uniform power profile (A2) and a cosine power profile (A4 and A8), A8 featuring in addition a central unheated thimble. The DNB location is given only in the A4 and A8 bundles. Only the DNB power is available in the A2 bundle. All tests of series 4 and 8 were run at the same pressure of 150 bars, while the range in series 2 spreads from 50 to 170 bars.

Some statistics of the simulation results (relative power : computed over data in % of experimental data) are given in the following table.

	Power	Central		average of calc. DNB	Std
Bundle	profile	thimble	Number of tests	power over data	deviation
A2	uniform	no	11	87.8%	17%
A4	cosine	no	20	78.4%	3.1%
A8	cosine	yes	24	81.8%	8.7%

Table 3: results of 3 series of DNB simulations in rod bundles

The results in the bundle A2 are weakened by two tests at very low flow rate, which are over predicted contrary to the 9 other tests; this enlightens the large value of the standard deviation for this bundle. A similar behaviour exists in series 4 and series 8 where the 2 tests at very low flow rate show significant differences (larger DNB power) compared to the other tests. Generally speaking, the height of the first detected DNB matches better in the series 4 than in the series 8.

The general underprediction of the DNB power in rod bundles may be linked to the use of look-up tables in a 3D analysis; such tables can predict CHF or DNB given 3 parameters: mass velocity, pressure and steam quality. These tables were built using 1D analysis of numerous tests. But in a 3D analysis, the code uses the locally calculated values of these 3 parameters: the steam quality and the mass velocity must obey a local definition with local void fraction and velocities and may display wrong values. As a consequence, the code computation of the local CHF may deviate from the recommended value. Better results can be expected when this point is improved.

4. Conclusion

The 1D and 3D modules of the CATHARE 3 system code were used for the simulations of PSBT benchmark tests. Results of void fraction, temperature measurements in Phase I and DNB power measurements in phase II have been compared to calculation results. The void comparison show that our models of wall and interfacial friction, coupled with void dispersion lead to satisfactory results, with a slight bias towards void underprediction, for both single subchannels and full rod bundles.

The exercise 1 of phase II, devoted to single phase mixing and cross flows in liquid phase, show good results as far as the experimental heat balance of the tests remain satisfactory.

In the exercise 2 of benchmark phase II, steady DNB simulations in 3 different rod bundles show significant underprediction of the critical power (20% bias), which could be partly due to a poor local CHF assessment. Further analysis of transient tests are planned to complete the full set of benchmark exercises.

5. Acknowledgments

This work was made in the frame of the development of the NEPTUNE project, which is jointly developed by the Commissariat à l'Energie Atomique et aux énergies alternatives (CEA, France) and Electricité de France (EDF) and also supported by the Institut de Radioprotection et de Sûreté Nucléaire (IRSN, France) and AREVA-NP.

6. References

- [1] P.Emonot, A.Souyri, J.L.Gandrille, F.Barré, "CATHARE 3: A new system code for thermal-hydraulic in the context of the NEPTUNE project", *Proceedings of NURETH 13 conference* (2009)
- [2] A. Rubin, A. Schoedel, M. Avramova, H. Utsuno, S. Bajorek, A. Velazquez-Lozada "OECD/NRC benchmark based on NUPEC PWR subchannel and bundle tests (PSBT) *Volume I:* Experimental Database and Final Problem Specifications", NEA/NSC/DOC(2010)1, November 2010.
- [3] M. Valette. "Analysis of boiling two phase flow in rod bundle for NUPEC BFBT Benchmark with 3-field NEPTUNE System code", *Proceedings of the* 12th International Topical Meeting on Nuclear Reactor Thermal Hydraulics (NURETH 12) Sheraton Station Square, Pittsburgh, Pennsylvania, USA, September 30-October 4, 2007.
- [4] M. Chandesris, G. Serre, P. Sagaut. "Macroscopic turbulence model for flow in porous media suited for channel, pipe and rod bundle flows", *International Journal of Heat and Mass Transfer*, **49** (2006), pp. 2739-2750
- [5] M. Chandesris, D. Jamet, "Derivation of jump conditions for the turbulence k-ε_model at a fluid/porous interface", *International Journal of Heat and Fluid Flow*, **30** (2009), 306-318.
- [6] M. Drouin, O. Grégoire, O. Simonin, A. Chanoine, "Macroscopic modeling of thermal dispersion for turbulent flows in channels", *International Journal of and Mass Transfer*, **53** (2010), 2206-2217.